Available online at www.sciencedirect.com
ScienceDirect
Talanta 74 (2008) 1271–1280
Talanta
www.elsevier.com/locate/talanta

Characterization of cobalt pigments found in traditional Valencian ceramics by means of laser ablation-inductively coupled plasma mass spectrometry and portable X-ray fluorescence spectrometry

J. Pérez-Arantegui [a], M. Resano [a,*], E. García-Ruiz [a], F. Vanhaecke [b], C. Roldán [c], J. Ferrero [c], J. Coll [d]

[a] *Departamento de Química Analítica, Universidad de Zaragoza, Pedro Cerbuna 12, E-50009 Zaragoza, Spain*
[b] *Department of Analytical Chemistry, Ghent University, Krijgslaan 281-S12, B-9000 Ghent, Belgium*
[c] *Instituto de Ciencia de los Materiales, Universidad de Valencia, P.O. Box 22085, E-46071 Valencia, Spain*
[d] *Museo Nacional de Cerámica y Artes Suntuarias "González Martí", C/ Poeta Querol 2, E-46002 Valencia, Spain*

Received 13 April 2007; received in revised form 25 August 2007; accepted 30 August 2007
Available online 8 September 2007

Abstract

In this work, a comparison of the performances of laser ablation-inductively coupled plasma mass spectrometry (LA-ICPMS) and portable X-ray fluorescence (XRF) spectrometry for the characterization of cobalt blue pigments used in the decoration of Valencian ceramics is presented. Qualitative data on the elemental composition of the blue pigments obtained using both techniques show a good agreement. Moreover, the results clearly illustrate that potters utilized different kinds of cobalt pigments in different historical periods.

While both techniques seem suitable for the proposed task, they show different strengths and weaknesses. Portable X-ray fluorescence spectrometry is a cheaper and totally non-destructive technique, capable of providing fast and reliable results at the mg g^{-1} level. LA-ICPMS, on the other hand, offers a much higher detection power and better spatial resolution, but its use results in some sample damage (sample consumption at the μg level), while it is a more expensive and non-portable technique.

Keywords: LA-ICPMS; XRF; Solid samples; Glaze; Cobalt pigments; Ceramic

1. Introduction

Natural pigments have been used since ancient times for coloring materials. Among these, cobalt pigments were already known in the Near and Middle Eastern Late Bronze Age [1–4] for the intense blue color they can induce in glass. Nevertheless, it seems they have been extensively used in glazes only since the Middle Ages [5]. Cobalt pigments were prepared from cobalt-rich minerals, such as cobaltite (CoAsS), erythrite ($Co_3(AsO_4)_2 \cdot 8H_2O$)), skutterudite ((Co, Ni)As_{3-x}) or asbolane ((Co, Ni)$_{1-y}(MnO_2)_{2-x}(OH)_{2-2y+2x} \cdot nH_2O$), or even cobaltiferous alum (a hydrated double sulfate that contains aluminum with or without another alkali, alkaline earth or transition metal). The latter was used to produce blue glass in New Kingdom Egypt [6–8].

Valencian ceramic workshops have manufactured blue-decorated glazed pottery since the 14th century AD in the areas of Paterna and Manises. The production of this type of ceramic continued until the 18th and 19th centuries, co-existing with the manufacturing of polychrome decorations [9]. Other colors, like green, brown or even metallic luster, were also used on Valencian ceramic. However, the likely local origin of the raw copper and manganese pigments, as well as their abundance in the Iberian Peninsula, make these pigments less suitable for the identification of different kinds of Valencian ceramic.

The chromatic characteristic of these decorated ceramics is an intense blue color, obtained by the application of the pigment (only cobalt compounds) over or under a white opacified glaze, mainly composed of tin oxide, lead oxide and silica. In general, traditional blue pigments fall into two distinct groups. The first group comprises the naturally occurring blue minerals, whilst the second group includes the blue compounds produced artificially from compounds usually having no obvious blue

* Corresponding author. Tel.: +34 976761634; fax: +34 976761292.
E-mail address: mresano@unizar.es (M. Resano).

0039-9140/$ – see front matter © 2007 Elsevier B.V. All rights reserved.
doi:10.1016/j.talanta.2007.08.044

characteristics in their raw unprocessed state in nature. Cobalt blue compounds occur only in the second group [10]. Thus, the elemental composition of the pigments is expected to depend both on the raw materials used and the workshop recipes, and it is important to establish the origin of the pigments as well as to investigate the temporal evolution of materials and techniques, although it is not always easy to discriminate between both sources of variation. The study of the pigment application technique [11], as well as the possible compositional differences between cobalt products used from the 14th to the 19th centuries, can bring about new insights on the technology and trade routes of raw materials related to Valencian ceramic production [12].

Trace element analysis can be particularly useful for the fingerprinting of art objects. Many analytical techniques can be used to reveal the trace chemical composition of archaeological samples. In the particular case of vitreous materials, the use of those techniques that provide information directly from the solid sample is recommended, taking into consideration the difficulties in dissolving this kind of sample and also having in mind the requirement of minimal sample damage. Among the different solid sampling techniques available, both X-ray fluorescence (XRF) spectrometry and laser ablation-inductively coupled plasma mass spectrometry (LA-ICPMS) can be particularly suitable to determine the elemental composition of glass and glazed ceramics [13–21]. Preliminary studies using both techniques [12,22] have demonstrated the presence of some characteristic elements in the blue pigments. These elements comprise arsenic, cobalt, copper, manganese and zinc. They might have been formerly present in the mineral ores used or were incorporated during the production of the ceramics. In any case, their presence can permit the classification of ceramic fragments according to period or workshop.

LA-ICPMS fulfills all the requirements (sufficient detection power, wide linear dynamic range and capabilities for spatially resolved analysis) demanded for these studies, providing multielemental results with no sample preparation, minimal sample damage and acceptable reproducibility and sample throughput. Applications of LA-ICPMS to investigate glazed ceramics are still scarce, but this approach is constantly gaining ground [22–27], mainly due to the availability of deep-UV laser systems that permit a more efficient ablation of this kind of samples [28,29]. On the other hand, energy dispersive X-ray fluorescence spectrometry (EDXRF) provides a non-destructive analytical technique and is widely applied for material analysis in Cultural Heritage investigations because of the possibility of in situ analysis by means of portable instrumentation and its high sample throughput (the analysis of a large number of objects or a high number of points in a object can be performed in a short time). EDXRF is a multi-element technique, allowing the fluorescence radiation of all of the elements with atomic number above $Z = 11$ (sodium) that are present in the object to be detected simultaneously, and it has already been used for a long time as an analytical tool to perform chemical analysis to determine major, minor and trace elements of historical objects [30]. In the field of glazed ceramic characterization, EDXRF analysis has permitted differentiation between two different types of decoration techniques: underglaze (where the pigment is applied on the fired clay body before the glaze application, whereafter clay body, pigment and glaze are subjected to a second firing process) and overglaze (where the raw glaze cover is applied on the previously fired clay body and then the pigment is applied directly on the top of the raw glaze cover, which vitrifies after a second firing process) [11]. Furthermore, this technique has allowed the identification of the chemical elements found in the compounds used in the production of the clay body, glaze and pigment decoration [12,31].

Also other solid sampling techniques, such as proton-induced X-ray emission spectrometry (PIXE), can provide useful analytical results on the elemental composition of this type of materials [16,32–35]. PIXE has been shown to be suitable for characterizing the elemental composition of different matrices, and some advantages of PIXE compared with other X-ray techniques are the higher sensitivity, the potential for spatially resolved analysis and the favorable excitation of light elements. Moreover, it is possible to implement this technique in the external beam mode (that is in air or in a helium atmosphere), enabling the analysis of large samples or of materials containing volatile compounds that would not stand vacuum conditions. [36]. But PIXE requires a particle accelerator and considerable operator skills. These prerequisites lead to high-operating expenses, making this technique unsuitable for most routine labs. For this reason, this work will focus on the comparison between two more widespread solid sampling techniques, EDXRF and LA-ICPMS, only. The possibilities of both techniques for the characterization of cobalt pigments found in Valencian ceramics dating from different periods will be discussed in detail and the results obtained with these techniques compared, with the aim of establishing consistent compositional differences that could allow the samples to be discriminated chronologically.

2. Experimental

2.1. Apparatus

EDXRF analyses were performed by means a portable spectrometer (see Fig. 1) with a palladium X-ray tube (EIS, Italy), working up to 38 kV–0.3 mA (the maximum values for the potential and current of the X-ray tube, respectively), and a 500 μm thick Si-PIN detector (XR-100 CR, AMPTEK Inc., USA), thermoelectrically cooled, with an energy resolution of 170–180 eV at 5.9 keV and an entrance beryllium window of 12.5 μm thickness. A multi-channel AMPTEK MCA Pocket was used to control data acquisition.

Direct analysis of ceramic fragments was also accomplished by using laser ablation (LA) for sample introduction. In the GeoLas ArF excimer-based LA system (MicroLas, Germany) used, the 193 nm UV-laser beam coming from the Compex102 laser unit (LambdaPhysik, Germany) undergoes homogenization [37], enabling flat-bottomed and straight-walled craters to be obtained. The ablation cell was coupled to the ICP torch of the ICPMS unit by means of a 3 mm internal diameter Tygon tubing and Ar was used as the carrier gas. All measurements were carried out using a Perkin-Elmer Sciex

Fig. 1. The portable EDXRF spectrometer used in this work.

DRC*plus* quadrupole-based ICP-mass spectrometer (Canada). Despite the availability of the dynamic reaction cell to overcome spectral interferences, all measurements were made in vented mode.

A JEOL (USA) JSM 6400 scanning electron microscope (SEM) was used for evaluation of the craters produced and for the quantitative determination of those elements (aluminum, lead, potassium, sodium, silicon and tin) present at higher levels (% level). The results obtained for these elements proved to be of little use for fingerprinting purposes. The SEM was equipped with a system for energy dispersive X-ray analysis, EDXA (Oxford Instruments, INCAx-sight), with ZAF correction.

2.2. Procedure for the characterization of the blue pigments by EDXRF

The EDXRF spectrometer used in this work has a light weight (10 kg including X-ray tube, X-ray detector, electronic modules and base tripod) and it is compact and easy-to-handle and hence, very well-suited for in situ and non-destructive analysis. The X-ray source is able to provide a collimated beam with a small diameter to analyze small areas or details on large objects, and the energy-dispersive detector system has an acceptable energy resolution (170–180 eV at 5.9 keV) for discriminating between adjacent X-ray fluorescence peaks. In this particular work, the X-ray beam was collimated down to 3 mm using aluminum pinholes. The ceramic samples were placed at the front of the measurement head with a 45° angle between the incident beam and the sample-detector, located at a distance of about 2 cm. EDXRF analyses were carried out, while operating the X-ray tube at a potential of 35 kV, a current intensity of 0.1 mA and an acquisition time of 300 s. With these parameters, fluorescence lines could be observed within a wide energy range and the EDXRF spectra were obtained with acceptable statistics. Prior to XRF analysis, the surface of the samples was cleaned with ethanol. Subsequently, XRF spectra were collected from three sampling points in colored zones and three sampling points in non-colored zones, to determine the composition of both the glaze and the pigment.

2.3. Procedure for the characterization of the blue pigments by LA-ICPMS

The parameters used during the analysis of the ceramics are presented in Table 1. Prior to analysis, the surface of the fragments was cleaned with diluted (0.14 M) HNO_3. In order to obtain representative values, for every ceramic fragment, fives sampling positions were selected across the glazed surface, ensuring focusing on the blue-colored (Co-enriched) areas, and each ablation consisted of 300 laser pulses. At every spot, the surface was first cleaned using 10 laser pulses of the same spot size to prevent the possible influence of any surface contamination or alteration. The analysis time per sample is approximately 5 min. The treatment of the transient signals generated was carried out as described elsewhere [38]. The signals for every nuclide were

Table 1
Instrumental operating conditions and data acquisition parameters for the LA-ICPMS measurements

GeoLas Laser ablation system	
Energy density	15.0 J cm^{-2}
Repetition rate	20 Hz
Spot size	120 μm
Number of cleaning pulses	10
Number of pulses for analysis	300 (15 s duration)
Cell volume	≈30 cm^3
ICP-mass spectrometer	
rf power	1200 W
Plasma argon flow rate	17 L min^{-1}
Auxiliary argon flow rate	1.2 L min^{-1}
Carrier argon flow rate	1.3 L min^{-1}
Sampling cone and skimmer	Platinum
Lens voltage	6.25 V
Data acquisition	
Scanning mode	Peak hopping
Dwell time per acquisition point	20 ms
Signals monitored[a]	$^{55}Mn^+$, $^{57}Fe^+$, $^{58}Ni^+$, $^{59}Co^+$, $^{65}Cu^+$, $^{68}Zn^+$, $^{75}As^+$, $^{209}Bi^+$ ($^{23}Na^+$), ($^{34}S^+$), ($^{35}Cl^+$)
Detector mode	Dual (pulse counting and analogue)

[a] Nuclides between parentheses were monitored only to assess the possible effect of interferences.

normalized to the signal of $^{59}Co^{+}$. In this way, five normalized signals were finally obtained for every element in every sample. The median of these five signals was taken as the representative value instead of the mean in order to minimize the possible influence of outliers [39–41]. This procedure was repeated on two different days for every sample to ensure consistency of the results.

3. Results and discussion

3.1. EDXRF measurements

Direct analysis of solid samples using a portable EDXRF spectrometer is very simple, because one just has to face the spectrometer to the surface of the object to be analyzed, and in a few minutes, the corresponding spectrum is obtained. However, the interpretation of the spectra is usually harder, due to the complexity of the sample composition. The main characteristics of this technique are summarized in Table 2, enabling comparison with those of LA-ICPMS.

The operating conditions chosen for EDXRF analysis (see Section 2.2.) provided detection limits of approximately 300 μg g^{-1} for those elements found in the periodic table between manganese ($Z=25$) and arsenic ($Z=33$) and of 1000 μg g^{-1} for elements between silver ($Z=47$) and tin ($Z=50$).

EDXRF analysis is generally based on an area of several mm^2 and a thickness between a few μm and a few mm, depending on the material under study and the surface conditions. In this case, the beam scans an area of 7 mm^2 and penetrates up to a depth of 100–200 μm under the superficial layer. The penetration depth of the X-ray beam was evaluated from the estimated total attenuation coefficient of the glaze cover for an exciting X-ray beam with an energy in the 5–20 keV interval and considering the typical average composition of tin-opacified lead glazes used in Spanish ceramics [42]. In glazed ceramic studies, the sample cross-section consists of a glazed external layer containing the pigment on top on a clay body; therefore, an EDXRF spectrum comprises information coming from these different layers due to the deep penetration of the X-rays in the sample. Discrimination between the characteristic elements of the pigment can be achieved by subtracting the EDXRF spectrum of a zone comprising glaze, pigment and ceramic body and the EDXRF spectrum of a zone comprising only glaze and ceramic body. From the net spectrum thus obtained, the characteristic elements of the pigments (arsenic, cobalt, copper, manganese and zinc) can be identified [12,43].

From the spectrum obtained for a blue pigment zone of about 7 mm^2, the net surface intensity of the Kα lines for the major elements cobalt, copper, manganese and zinc was calculated for each sample. For arsenic, on the other hand, the Kβ line was used instead, since its Kα line overlaps with the Pb Lα line. The calculation of the net peak intensities and the deconvolution of the fluorescence line pairs Mn Kβ/Fe Kα, Fe Kβ/Co Kα, Ni Kβ/Cu Kα and Cu Kβ/Zn Kα, were performed using the WinQXAS code [44]. Also other elements, such as iron and nickel, have been monitored, but these have not been included in the discussion, as they did not contribute significantly to the pigment discrimination. Lead has not been considered among the possible characteristic elements of the pigment because it is not possible to discriminate whether the fluorescence lines come from the pigment or from the glaze cover, in which it is very abundant due to its use as melting agent.

The use of certified standards or ceramic sherds of known composition for calibration could have been checked in order

Table 2
Comparison of the main characteristics of both solid sampling techniques discussed in this work

	LA-ICPMS	XRF
Types of samples	All Preparation of tablets for powders is required Decreasing the fragment size to fit into the ablation cell may be required	All Preparation of tablets for powders may be required
Usual working range	100 ng g^{-1} to wt%	100 μg g^{-1} to wt%
Precision	5–25%	1–5%
Selectivity	Medium–high[a]	Medium[b]
Calibration	Solid standards with an internal standard	Solid standard reference materials
Isotopic analysis	Yes	No
Multi-element potential	Yes	Yes
Sample throughput	2–5 min per sample	1–5 min per sample
Sample Consumption	100 ng–10 μg	None
Spatial resolution		
Lateral	Very good (μm)	Very poor (several mm^2)
In depth	Excellent (≈0.1 μm)	Poor (μm to mm)
Automation availability	No	No
Portability	No	Yes
Prices	From 250,000€[a]	From 30,000€[b]

[a] This aspect greatly depends on the type of mass analyzer used; with sector field instead of the more traditional quadrupole-based instrumentation the selectivity is greatly improved. On the other hand, the use of collision/reaction cells, located in-between the interface and the quadrupole mass analyzer can also bring about a significant improvement.

[b] Depends on the characteristics of the X-ray tube and the semi-conductor detector.

to obtain quantitative results. However, quantification was not attempted at, because obtaining reliable results is a difficult task due to both irregularities in the thickness of the analyzed surface layers and compositional heterogeneities. In fact, obtaining bulk information may even not be not very meaningful for fingerprinting purposes in this case, since the concentration of many elements may strongly depend on the amount of pigment added to the sample; even for one particular sample, the content may significantly vary in different sections depending on the coloration, as dark blue areas contain higher amounts of pigment that pale blue areas. Since all of the blue pigments used in the ceramic samples investigated in this work have been obtained from cobalt mineral ores, the signal for this element provides an indication of the amount of pigment added. Thus, the peak area ratios between the XRF lines of the detected elements (Mn Kα, Cu Kα, Zn Kα, As Kβ) and the line Co Kα might be considered as a guide to the source of the ore from which the colorant was derived and, thus, this parameter is more suitable to discriminate between different types of pigments.

3.2. LA-ICPMS measurements

The principle of the technique is based on the use of a short laser pulse (typically a few nanoseconds) that delivers a burst of energy to the sample surface. As a consequence, a small amount of material is ablated and the aerosol thus formed is transported by means of a gas (Ar in this work) flow into the ICPMS instrument for elemental and/or isotopic monitoring [28,29]. The main characteristics of this technique are summarized in Table 2.

This technique cannot be considered as entirely non-destructive, but the damage produced to the sample is very limited. Moreover, the technique allows spatial information to be obtained, both laterally and/or in depth. With the instrumentation used in this work, the laser beam diameter can be varied between 4 and 120 μm, giving rise to almost regular circular craters with radius ranging between 2 and 60 μm. The use of a large spot size results in more material ablated and thus, a higher sensitivity (which shows a linear dependence with the square of the radius), but also in more damage inflicted to the sample. In this work, a spot size of 120 μm was selected for maximizing the sensitivity. On the other hand, also the number of pulses used per sampling spot can be varied. Selecting a high number of pulses permits obtaining a more representative value, but it is necessary to ensure that only the upper layer containing the cobalt pigment is ablated since the main goal of the study is to investigate the characteristics of these cobalt pigments. This could be easily assured by monitoring the $^{59}Co^{+}$ signal (in addition to the final examination of the craters by SEM). An ablation time of 15 s (corresponding to 300 laser pulses) was finally chosen. This 300 laser-pulse ablation results in a crater depth of ≈25 μm (estimated using SEM), which represents approximately 1 μg of sample ablated per spot. This value can be further reduced if needed for other materials, but only at the cost of deteriorated LODs. For the samples investigated in the present work, these parameters are perfectly acceptable as the craters thus produced are hardly noticeable by visual observation.

Other important parameters for the ablation (repetition rate and the energy density), and some important ICPMS settings—the carrier gas flow rate that determines the transport efficiency from the ablation chamber to the ICPMS and the rf power that has an important influence on the sensitivity, were optimized aiming at maximum signal intensities for the target elements. The maximum repetition rate (20 Hz) available with the laser unit used was chosen. As to the energy output, no significant gain in sensitivity was obtained above ∼1.5 mJ (energy measured on the substrate, corresponding with an energy density of 13.3 J cm^{-2}). Finally, a value of 1.7 mJ (energy density 15.0 J cm^{-2}) was selected. All the settings finally used are summarized in Table 1.

The elements monitored in this study were selected based on the information available from a previous work, in which ceramic materials from a different Spanish region (Aragón) were investigated [22]. The conclusion of that work was that arsenic, copper, manganese and zinc provide the most relevant information for discriminating purposes. Other elements, such as iron, nickel and bismuth, were simultaneously monitored in order to check if more information could be obtained. Experiments were carried out to ensure that these elements could be monitored interference-free. The signal intensities observed for $^{35}Cl^{+}$ were practically irrelevant (glazed ceramics from this region are expected to show a low content of this element), therefore enabling the monitoring of $^{75}As^{+}$ with no risk of interference from $^{40}Ar^{35}Cl^{+}$. Due to the high-signal intensity encountered for $^{23}Na^{+}$ (which could be anticipated for a vitreous surface) on the other hand, the monitoring of the less abundant $^{65}Cu^{+}$ nuclide was preferred (overlap of the signals of $^{63}Cu^{+}$ and $^{40}Ar^{23}Na^{+}$). A less abundant isotope of zinc (^{68}Zn) was also selected to minimize the possible effect of sulfur-based polyatomic ions (overlap of the signals of $^{64}Zn^{+}$ and $^{66}Zn^{+}$ with those of $^{32}S^{16}O_2{}^{+}$ and/or $^{32}S^{32}S^{+}$ and $^{34}S^{16}O_2{}^{+}$ and/or $^{32}S^{34}S^{+}$, respectively). Table 1 shows the nuclides finally monitored for all the samples under investigation.

A typical signal profile obtained when ablating the same sample at five different locations and using the conditions summarized in Table 1 is presented in Fig. 2a. It appears that it is possible to achieve a controlled ablation of the sample, since the signals for all of the elements remain very stable (the R.S.D. ranged between 3 and 10%, values that can be further reduced to 2–5% when the respective signals are normalized to the $^{59}Co^{+}$ signal). Regular, flat-bottomed craters were observed by means of SEM in all cases, proving the suitability of the 193 nm ArF laser unit for efficient ablation of the vitreous surface of the ceramic samples, as can be appreciated in Fig. 2b.

The sensitivity of the technique permitted to obtain significant signals for all of the elements investigated in every sample. Limits of detection of 0.06 (arsenic), 0.02 (cobalt), 0.07 (copper), 0.06 (manganese) and 0.3 (zinc) μg g^{-1} were calculated (IUPAC 3s-criterion, using the gas blank). Even though it might be feasible to obtain quantitative information by means of calibration against a suitable standard (typically the NIST 610-617 series) and using the signal for an element of known concentration as internal reference (frequently an element present at a high level that can be determined using a less sensitive solid sam-

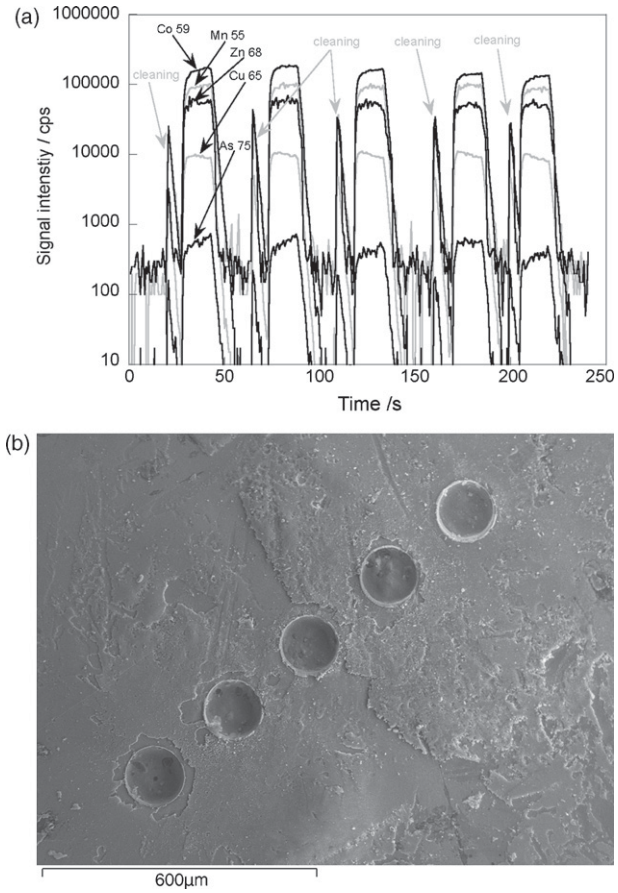

Fig. 2. (a) Signal intensity *vs*. time profiles obtained upon ablation of the glazed layer of a ceramic sample (GSM1). The cleaning period is not considered for quantification purposes. (b) Secondary electron image of the five craters produced by laser ablation.

pling technique, such as SEM), the goal of the study was not to obtain quantitative information, but rather enable discrimination between the different pigments used through the years. In fact, as already discussed in the previous section, since the amount of cobalt pigment that was added can differ very significantly from one sample to the other and even within one sample, bulk analysis of the glazed layers can hardly result in the establishment of any clear pattern. Instead, it was preferred to normalize the intensity values for all the nuclides monitored to the signal of $^{59}Co^{+}$, since this signal is directly related to the amount of pigment added. It was this parameter (the signal for every nuclide relative to the cobalt signal) that was finally used in order to look for possible differences among samples.

3.3. Characterization of the Valencian blue pigments

Ten ceramic fragments from the collection of the *Museo Nacional de Cerámica y Artes Suntuarias González Martí* (Valencia, Spain), with cobalt pigment decoration, were analyzed by EDXRF and LA-ICPMS. In Fig. 3, these samples are shown, while the corresponding caption offers a short description of the characteristics and the results of dating of the samples by experts using a traditional approach, based on stylistic and historical considerations.

Fig. 4 shows the ratio between the net intensities of the XRF lines of the selected elements (arsenic, manganese, copper, and zinc) and the net intensity of the Co Kα line. Cobalt was found in all the pigment samples analyzed. Copper and manganese were detected in the blue pigment of all of the ceramic samples in a relatively wide range of concentrations. Zinc was always detected, but was only found in a high concentration in the sample of the 14th century. This shows that, before the 15th century, the cobalt pigment was produced from cobalt ores probably extracted together with zinc blend [46]. The presence of arsenic was not detected in samples from the 14th and 15th century and in the samples Co29 (17th century) and GMS20 (19th century). This is an indication of the use of cobalt pigments with a very low-arsenic concentration ($<LOD_{XRF}$).

Fig. 5 shows the LA-ICPMS results of the more characteristic elements (arsenic, manganese, copper, and zinc), also expressed as normalized intensities, in order to distinguish chronological features. The results for other measured elements, like nickel, iron, or bismuth, have not been incorporated because they do not add any new discriminating information. Nickel and iron show a good correlation with the cobalt content ($r > 0.95$), and bismuth seems to be correlated with arsenic, so they do not significantly help to establish new differences among any group of samples. One of the advantages of the use of LA-ICPMS for this characterization is the better sensitivity attained, resulting in much improved limits of detections (see Section 3.2.), which can be particularly relevant for elements that are present at low levels in some of the samples, like arsenic. Owing to the very good spatial resolution (crater dimensions: 120 μm diameter and 25 μm depth), elements coming from the clay body do not affect the results obtained.

In general, the analytical results obtained by means of both techniques show a good agreement, leading to similar conclusions. It can be mentioned that it is not really meaningful to directly compare the signal intensity ratios obtained for every element with both techniques. Differences are expected owing to the different relative sensitivity of the analytes when using LA-ICPMS or XRF, particularly considering that the conditions selected are not always those corresponding to maximum signal intensity, but to a lower risk of interferences (e.g., when selecting the nuclides monitored or the emission lines). Moreover, the less homogeneous distribution of an element in one particular pigment may be the source for some discrepancies, owing to the very different amount of sample that is analyzed with these techniques. Furthermore, the reliability of the results obtained with XRF for samples with low-cobalt content (very pale blue samples, in which the cobalt signal might be close to the LOD) is lower and may give origin to some artificially high ratios (e.g., sample Co29). In spite of these considerations, what is relevant to stress is that very similar trends in the ratios were observed with both techniques, indicating that is possible to differentiate the Valencian samples chronologically because of the use of different cobalt pigments. The first noticeable pigment feature is higher arsenic contents from the 16th century up to the 18th century AD. Earlier samples (14th and 15th century) have very low proportions (see Fig. 4). This difference was already noted in previous papers [12,22] and also for other

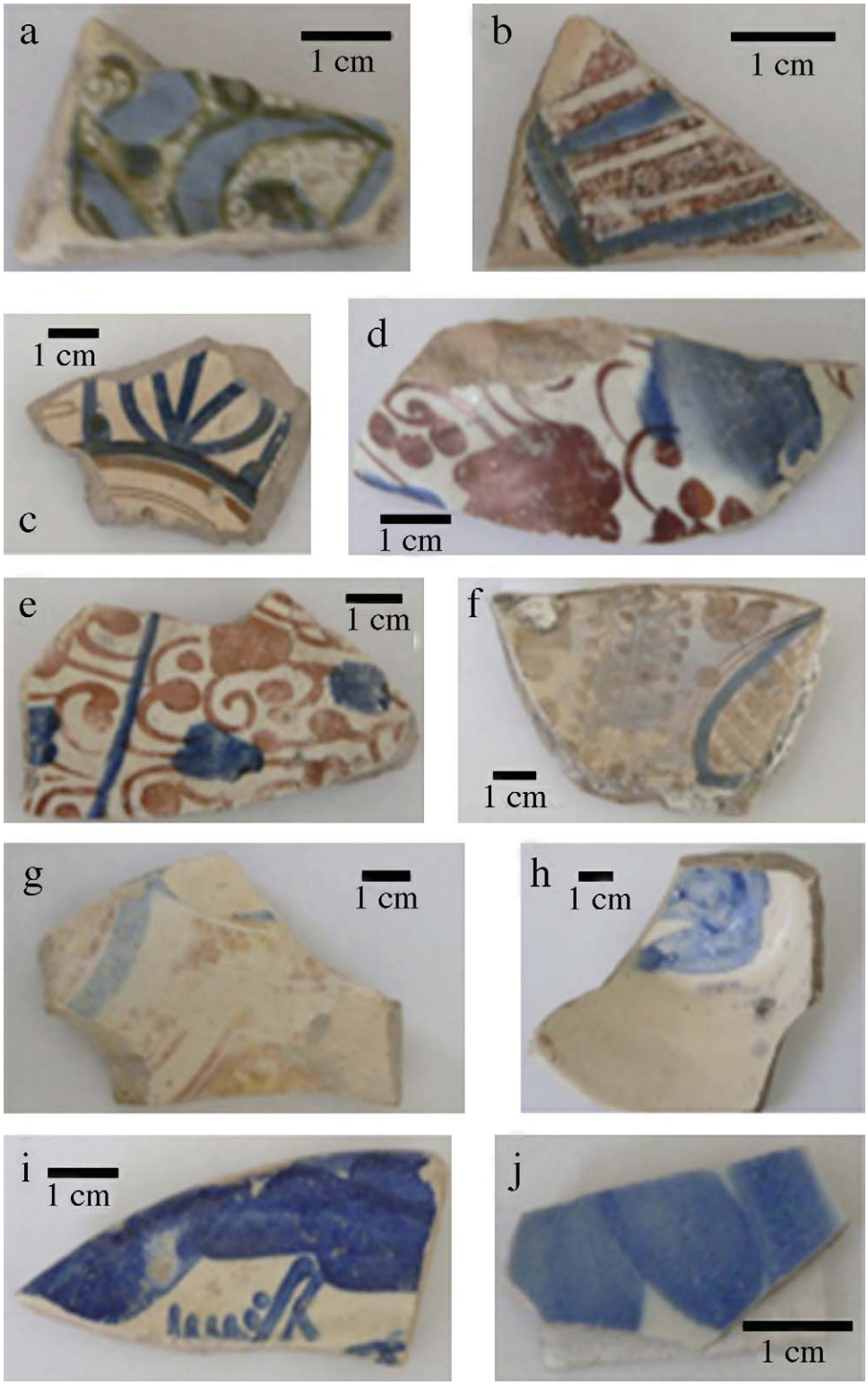

Fig. 3. (a) Sample GMS1, fragment of vase in Malaga style, century. 1330–1370. (b) Sample C124, fragment of bowl in Pula style with radial metopes, century 1380–1410. (c) Sample GMS6, fragment of bowl of the crown series, century 1410–1425. (d) Sample GMS9, fragment of "ivy leaf" vase, century 1450–1480. (e) Sample GMS10, fragment of "ivy leaf" vase, century 1475–1500. (f) Sample GMS11, fragment of bowl with scallop and lobed leaves, century 1580–1600. (g) Sample GMS12, fragment of dish edge with reserved elements, century 1600–1610. (h) Sample Co29, fragment of bowl with a blue fringed leaf, century 1650–1675. (i) Sample Co36, fragment of deep dish with decoration of hangings, century 1780. (j) Sample GMS20, a typical fragment of closed vessel, century 1850. All of the samples originate from Manises-Paterna workshops (Valencia, Spain). (For interpretation of the references to color in this figure legend, the reader is referred to the web version of the article.)

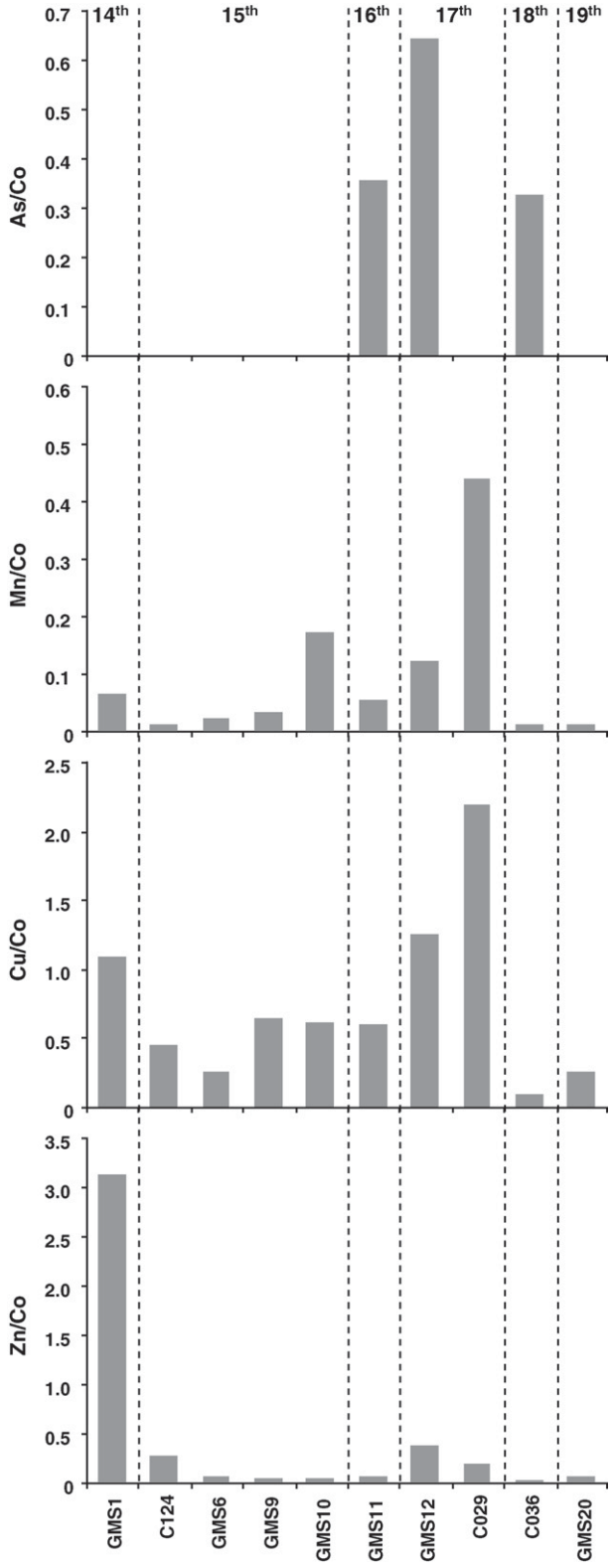

Fig. 4. Co-normalized intensities of the XRF lines of the selected elements detected in Valencian ceramic samples with cobalt-blue decoration. Histograms represent the ratios of the following signal intensities As Kβ/Co Kα, Mn Kα/Co Kα, Cu Kα/Co Kα and Zn Kα/Co Kα.

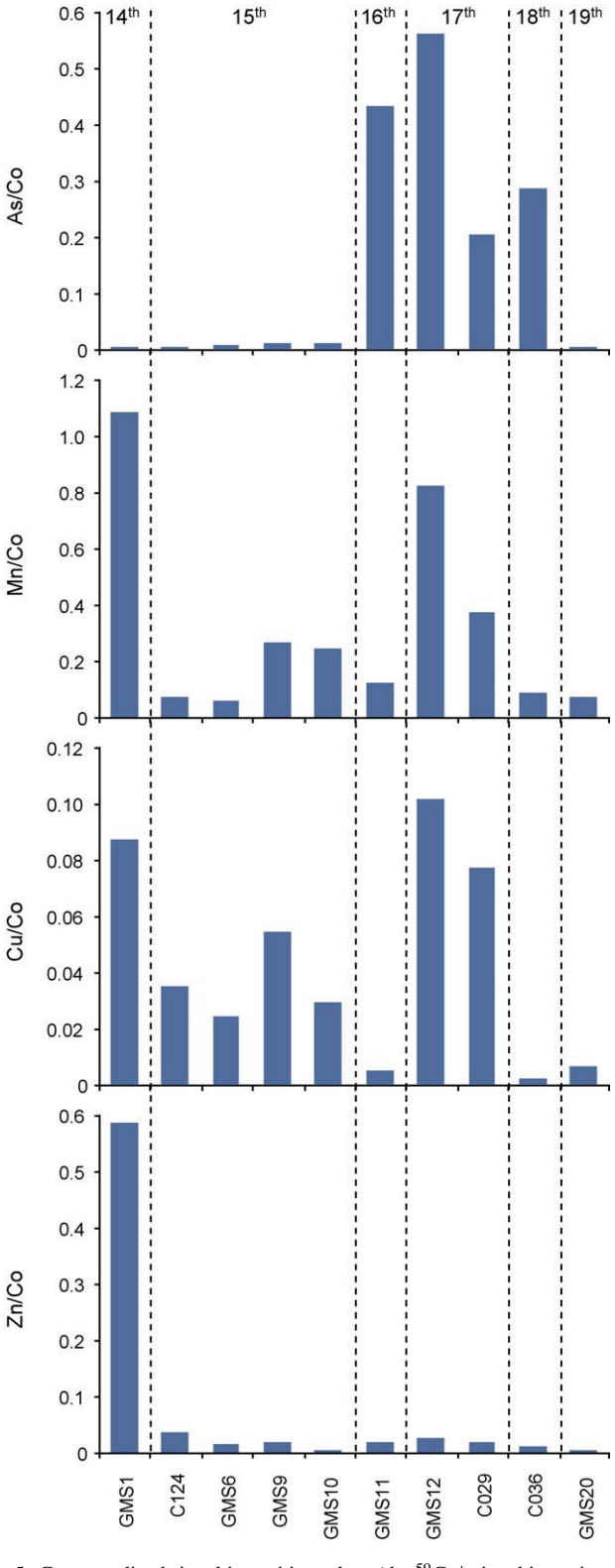

Fig. 5. Co-normalized signal intensities values (the $^{59}Co^{+}$ signal intensity was chosen as internal reference) for the elements of interest (^{75}As, ^{55}Mn, ^{65}Cu and ^{68}Zn) in blue decoration of Valencian ceramics, as obtained using LA-ICPMS.

blue-decorated ceramic materials [16,45]. Some authors even date this technological change more specifically between 1517 and 1520 [35]. Higher arsenic contents suggest that the pigment used in the samples could have been linked to minerals like cobaltite (CoAsS), erythrite ($[Co, Ni]_3[AsO_4]_2 \cdot 8H_2O$), smaltite ($[Co, Ni]As_{3-2}$) or skutterudite ($(Co, Ni)As_{3-x}$). The presence of arsenic in the blue pigments from the 16th century in glass and glazes from different regions (e.g., Italy, France and Spain) could be explained by the use of a new cobalt source or a different technology for obtaining cobalt from the mineral ores [35,45,46]. The fact that Spanish blue-decorated ceramics also show this change [12,22] would prove that there was a European technological event, not exclusive to some countries, in the use of cobalt pigments. The low arsenic proportions in the 19th century sample already suggest the more recent use of very pure cobalt pigments.

Two other characteristic elements are manganese and copper, with higher proportions in the 14th and the 17th century, and medium levels of copper in the 15th century. Zinc is only present in higher quantities in 14th century samples, as already noted in previous studies [12]. In this way, Valencian ceramics can be characterized by the use of different blue-pigment compositions during several periods: 14th century samples are characterized by an association of Co–Zn–Cu, 15th century samples by the combination of Co–Cu (with an increasing amount of manganese for samples corresponding to the late 15th century), 16th century samples by that of Co–As, 17th century samples by the combined presence of Co–As–Cu–Mn, 18th century samples by Co–As, and 19th century samples by the use of very pure cobalt. The latter purity could either suggest a change in pigment-supply or technological changes, but it also provides a most important chronological distinction.

4. Conclusions

The use of EDXRF and LA-ICPMS techniques has enabled to characterize the blue pigments of some selected Valencian ceramic fragments from the *Museo Nacional de Cerámica y Artes Suntuarias González Martí* (Valencia, Spain). EDXRF and LA-ICPMS results are in good agreement and similar conclusions can be extracted from the measurement data. Elemental information corresponding to arsenic, copper, manganese and zinc allow characteristic blue pigments from several periods to be distinguished from one another, proving that potters used different kinds of cobalt materials in several centuries and suggesting changes in pigment-supply or technological changes in the extraction of cobalt from the ore(s). Both techniques seem fit-for-purpose in this case, although they show different advantages and drawbacks: portable X-ray fluorescence spectrometry is an inexpensive and non-destructive technique, capable of providing results at the $mg\,g^{-1}$ level in a very fast way. LA-ICPMS, on the other hand, is a non-portable and more expensive technique that provides a superior detection power and a much better spatial resolution, both laterally and in depth, although its use results in some sample damage (μg level or lower).

Acknowledgements

This study was financially supported by CTPP03/2005 research project of the "Comunidad de Trabajo de los Pirineos" (Aragon-Catalonia-Aquitaine) and by the Diputación General de Aragón (DGA), Research Projects PM081/2006 and PM013/2007, and also by the Ministerio de Ciencia y Tecnología (projects Ref. BHA2003-05800 and CTQ2006-03649). Martín Resano acknowledges the Spanish Ministry of Science and Education (Secretaría de Estado de Universidades e Investigación, Programa Nacional de Ayudas para la Movilidad de Profesores de Universidad) and Esperanza García-Ruiz the 'Europa' program from CAI and DGA (CONSI + D; Grant reference CB13/05) for financially supporting their stay at Ghent University.

References

[1] A. Kaczmarczyk, R.E.M. Hedges, Ancient Egyptian Faience, Aris & Phillips, Warminster, 1983.
[2] C. Pulak, in: S. Swiny, R. Hohlfelder, H. Swiny (Eds.), Res Maritimae: Cyprus and the Eastern Mediterranean from Prehistory to Late Antiquity, Scholars Press, Atlanta, GA, 1997, pp. 233–262.
[3] T. Rehren, E.B. Pusch, J. Egypt. Archaeol. 83 (1997) 127–141.
[4] T. Rehren, Archaeometry 39 (1997) 355–368.
[5] Y. Porter, La céramique médiévale en Méditerranée, Actes du 6e congrès, Narration éditions, Aix-en-Provence, 1997 pp. 505–512.
[6] A. Kaczmarczyk, in: J.S. Olin, M.J. Blackman (Eds.), Proceedings of the 24th International Archaeometry Symposium, Smithsonian Institution Press, Washington, DC, 1986, pp. 369–376.
[7] A.J. Shortland, M.S. Tite, Archaeometry 42 (2000) 141–151.
[8] A.J. Shortland, M.S. Tite, I. Ewart, Archaeometry 48 (2006) 153–168.
[9] J. Coll, El azul en la loza de la Valencia medieval, Catálogo de la Exposición, Valencia, 1995.
[10] J.R. Taylor, Sci. Archaeol. 19 (1977).
[11] C. Roldán, J. Coll, J.L. Ferrero, D. Juanes, Xray Spectrom. 33 (2004) 28–32.
[12] C. Roldán, J. Coll, J. Ferrero, J. Cult. Herit. 7 (2006) 134–138.
[13] K.N. Yu, J.M. Miao, Xray Spectrom. 28 (1999) 19–23.
[14] Ph. Colomban, G. Sagon, L.Q. Huy, N.Q. Liem, L. Mazerolles, Archaeometry 46 (2004) 125–136.
[15] R. Padilla, O. Schalm, K. Janssens, R. Arrazcaeta, P. Van Espen, Anal. Chim. Acta 535 (2005) 201–211.
[16] G. Pappalardo, E. Costa, C. Marchetta, L. Pappalardo, F.P. Romano, A. Zucchiatti, P. Prati, P.A. Mandò, A. Migliori, L. Palombo, M.G. Vaccari, J. Cult. Herit. 5 (2004) 183–188.
[17] T. Trejos, J.R. Almirall, Talanta 67 (2002) 396–401.
[18] T. Trejos, J.R. Almirall, Talanta 67 (2002) 388–395.
[19] C. Latkoczy, S. Becker, M. Ducking, D. Gunther, J.A. Hoogewerff, J.R. Almirall, J. Buscaglia, A. Dobney, R.D. Koons, S. Montero, G.J.Q. van der Peijl, W.R.S. Stoecklein, T. Trejos, J.R. Watling, V.S. Zdanowicz, J. Forensic Sci. 50 (2005) 1327–1341.
[20] D.N. Papadopoulou, G.A. Zachariadis, A.N. Anthemidis, N.C. Tsirliganis, J.A. Stratis, Spectrochim. Acta B 59 (2004) 1877–1884.
[21] I. De Raedt, K. Janssens, J. Veeckman, L. Vincze, B. Vekemans, T.E. Jeffries, J. Anal. At. Spectrom. 16 (2001) 1012–1017.
[22] M. Resano, J. Pérez-Arantegui, E. García-Ruiz, F. Vanhaecke, J. Anal. At. Spectrom. 20 (2005) 508–514.
[23] H. Neff, J. Archaeol. Sci. 30 (2003) 21–35.
[24] R.J. Speakman, H. Neff, Am. Antiquity 62 (2002) 137–144.
[25] B. Gratuze, M. Blet-Lemarquand, J.N. Barrandon, J. Radioanal. Nucl. Chem. 247 (2001) 645–656.
[26] D.V. Hill, R.J. Speakman, M.D. Glascock, Archaeometry 46 (2004) 585–605.
[27] E.E. Cochrane, H. Neff, J. Archaeol. Sci. 33 (2006) 378–390.
[28] D. Günther, B. Hattendorf, Trends Anal. Chem. 24 (2005) 255–265.

[29] R.E. Russo, X. Mao, H. Liu, J. Gonzalez, S.S. Mao, Talanta 57 (2002) 425–451.
[30] E. Selin (Ed.), Special Millennium Issue on Cultural Heritage, X-ray Spectrom, vol. 29, 2000.
[31] K.N. Yu, in: D.C. Creagh, D.A. Bradley (Eds.), Radiation in Art and Archaeometry, Elsevier, 2000, pp. 317–346.
[32] A. Zucchiatti, A. Bouquillon, J. Salomon, J.R. Gaborit, Nucl. Instrum. Meth. Phys. Res. B 161–163 (2000) 699–703.
[33] A. Bouquillon, J. Castaing, E. Vartanian, A. Zink, A. Zucchiatti, in: J.R. Gaborit, M. Bormand (Eds.), Les della Robbia: Sculptures en Terre Cuite Émaillée de la Renaissance Italienne, Rèunion des Musées Nationaux, Paris, 2002, pp. 139–158.
[34] I. Biron, S. Beauchoux, Meas. Sci. Technol. 14 (2003) 1564–1578.
[35] A. Zucchiatti, A. Bouquillon, I. Katona, A. D'Alessandro, Archaeometry 48 (2006) 131–152.
[36] J.-C. Dran, T. Calligaro, J. Salomon, in: E. Ciliberto, G. Spoto (Eds.), Chemical Analysis Series, vol. 155, John Wiley Sons, 2000.
[37] D. Günther, R. Frischknecht, C.A. Heinrich, H.J. Kahlert, J. Anal. At. Spectrom. 12 (1997) 939–944.
[38] H.P. Longerich, S.E. Jackson, D. Günther, J. Anal. At. Spectrom. 11 (1996) 899–904.
[39] M.A. Belarra, M. Resano, J.R. Castillo, J. Anal. At. Spectrom. 14 (1999) 547–552.
[40] M. Resano, F. Vanhaecke, D. Hutsebaut, K. De Corte, L. Moens, J. Anal. At. Spectrom. 18 (2003) 1238–1242.
[41] F. Vanhaecke, M. Resano, E. Garcia-Ruiz, L. Balcaen, K.R. Koch, K. McIntosh, J. Anal. At. Spectrom. 19 (2004) 632–638.
[42] M. Vendrell, J. Molera, M.S. Tite, Archaeometry 42 (2000) 325–340.
[43] J. Molera, T. Pradell, M. Mesquida, M. Vendrell, in: M. Mesquida (Ed.), Las Ollerías de Paterna, Tecnología y Producción, Ayuntamiento de Paterna, 2001, pp. 235–261.
[44] R. Capote, E. López, E. Mainegra, WinQXAS Manual (Quantitative X-Ray Analysis System for Widows) Version 1.2, IAEA, 2000.
[45] B. Gratuze, I. Soulier, M. Blet, L. Vallauri, Revue d'Archéometrie 20 (1996) 77–94.
[46] J. Hartwig, Verre 7 (2001) 40–48.